Molecular Modeling of the Human $P2Y_2$ Receptor and Design of a Selective Agonist, 2′-Amino-2′-deoxy-2-thiouridine 5′-Triphosphate

Andrei A. Ivanov,[†,‡] Hyojin Ko,[†,‡] Liesbet Cosyn,[§] Savitri Maddileti,[#] Pedro Besada,[†] Ingrid Fricks,[#] Stefano Costanzi,[||] T. Kendall Harden,[#] Serge Van Calenbergh,[§] and Kenneth A. Jacobson*[,†]

Molecular Recognition Section, Laboratory of Bioorganic Chemistry, National Institute of Diabetes and Digestive and Kidney Diseases, National Institutes of Health, Bethesda, Maryland 20892, Laboratory for Medicinal Chemistry, Faculty of Pharmaceutical Sciences (FFW), Ghent University, Harelbekestraat 72, B-9000 Ghent, Belgium, Department of Pharmacology, University of North Carolina School of Medicine, Chapel Hill, North Carolina 27599, and Laboratory of Biological Modeling, National Institute of Diabetes and Digestive and Kidney Diseases, National Institutes of Health, Bethesda, Maryland 20892

Received July 28, 2006

A rhodopsin-based homology model of the nucleotide-activated human $P2Y_2$ receptor, including loops, termini, and phospholipids, was optimized with the Monte Carlo multiple minimum conformational search routine. Docked uridine 5′-triphosphate (UTP) formed a nucleobase $\pi-\pi$ complex with conserved Phe3.32. Selectivity-enhancing 2′-amino-2′-deoxy substitution interacted through π-hydrogen-bonding with aromatic Phe6.51 and Tyr3.33. A "sequential ligand composition" approach for docking the flexible dinucleotide agonist Up_4U demonstrated a shift of conserved cationic Arg3.29 from the UTP γ position to the δ position of Up_4U and Up_4 ribose. Synthesized nucleotides were tested as agonists at human P2Y receptors expressed in 1321N1 astrocytoma cells. 2′-Amino and 2-thio modifications were synergized to enhance potency and selectivity; compound **8** ($EC_{50} = 8$ nM) was 300-fold $P2Y_2$-selective versus $P2Y_4$. 2′-Amine acetylation reduced potency, and trifluoroacetylation produced intermediate potency. 5-Amino nucleobase substitution did not enhance $P2Y_2$ potency through a predicted hydrophilic interaction possibly because of destabilization of the receptor-favored Northern conformation of ribose. This detailed view of $P2Y_2$ receptor recognition suggests mutations for model validation.

Introduction

P2 nucleotide receptors are activated by a range of naturally occurring extracellular nucleotides and consist of two families: the eight subtypes of P2Y receptors, which are G-protein-coupled receptors (GPCRs) ($P2Y_1$, $P2Y_2$, $P2Y_4$, $P2Y_6$, $P2Y_{11}$, $P2Y_{12}$, $P2Y_{13}$, and $P2Y_{14}$), and the seven subtypes of P2X ligand-gated cation channels.[1−5] The $P2Y_2$ receptor is activated by endogenous uridine 5′-triphosphate (UTP **1**), adenosine 5′-triphosphate (ATP **2**), and various dinucleotides (Chart 1). It is preferentially G_q-coupled and stimulates phospholipase Cβ (PLCβ). The $P2Y_2$ receptor, first cloned from mice,[6] is expressed in epithelial cells, smooth-muscle cells, endothelial cells, leukocytes, osteoblasts, and cardiomyocytes. In the central nervous system, activation of the receptor is associated with neuronal differentiation.[7] The $P2Y_2$ receptor appears to interact with integrins to stimulate chemotaxis and to enhance α-secretase-dependent amyloid precursor protein processing.[8,9] Activation of the $P2Y_2$ receptor causes a pronociceptive effect.[10] Agonists of the $P2Y_2$ receptor are of interest in the development of therapeutic agents for pulmonary diseases (e.g., cystic fibrosis), salivary gland dysfunction, and ophthalmic diseases.[11,12]

The SAR (structure−activity relationship) of nucleotides in activating the human $P2Y_2$ receptor has been probed.[2,3,13] UTP-γ-S **3** and the dinucleoside tetraphosphates INS365 (Up_4U) **4a** and INS37217 (Up_4dC) **4b** are potent and relatively stable agonists of the $P2Y_2$ receptor.[11,14]

The first site-directed mutagenesis and molecular modeling of transmembrane helical domains 6 and 7 (TMs 6 and 7) of the $P2Y_2$ receptor were reported by Erb et al.[15] Modeling methods have subsequently undergone significant development. Furthermore, a variety of newly synthesized potent analogues of UTP are available for docking studies. Hence, in the present study, we carried out new molecular modeling studies to predict sites of interaction of the ligands with the $P2Y_2$ receptor and to provide hypotheses for the design of additional analogues. Our recent publications[1,13] provided an initial rhodopsin-based homology model, which was refined in the present study. We also have optimized agonist selectivity for the $P2Y_2$ receptor by synthesizing new UTP analogues, which bear modifications at the uracil moiety and the ribose ring. Thus, this study integrates the synthesis of a highly selective agonist with modeling studies that use a molecular dynamics (MD) simulation in a phospholipidic and aqueous environment to refine the receptor and a Monte Carlo approach to ligand docking.

Results and Discussion

1. Structure of the $P2Y_2$ Receptor. A molecular model of the $P2Y_2$ receptor was recently published.[1] In contrast to the earlier model constructed by Erb et al.,[15] this model of the $P2Y_2$ receptor is a rhodopsin-based homology model containing not only seven TMs but also all extracellular and intracellular hydrophilic loops. Here, we present a further refined model of the $P2Y_2$ receptor, updated by insertion of a segment of the carboxyl-terminal (CT) domain including the H8 helix (Gly310−Met346) and the amino-terminal (NT) domain. The formal geometry of the model was tested with the ProTable command of Sybyl as well as the Procheck software (Supporting Information).[16]

* To whom correspondence should be addressed. Phone: 301-496-9024. Fax: 301-480-8422. E-mail: kajacobs@helix.nih.gov.
[†] Laboratory of Bioorganic Chemistry, National Institute of Diabetes and Digestive and Kidney Diseases.
[‡] These authors contributed equally to this work.
[§] Ghent University.
[#] University of North Carolina School of Medicine.
[||] Laboratory of Biological Modeling, National Institute of Diabetes and Digestive and Kidney Diseases.

10.1021/jm060903o CCC: $37.00 © 2007 American Chemical Society
Published on Web 02/16/2007

Chart 1. Structures of Native Nucleoside 5′-Triphosphate (UTP and ATP) Ligands and a Dinucleotide (Up_nU) Ligand of the $P2Y_2$ Receptor[a]

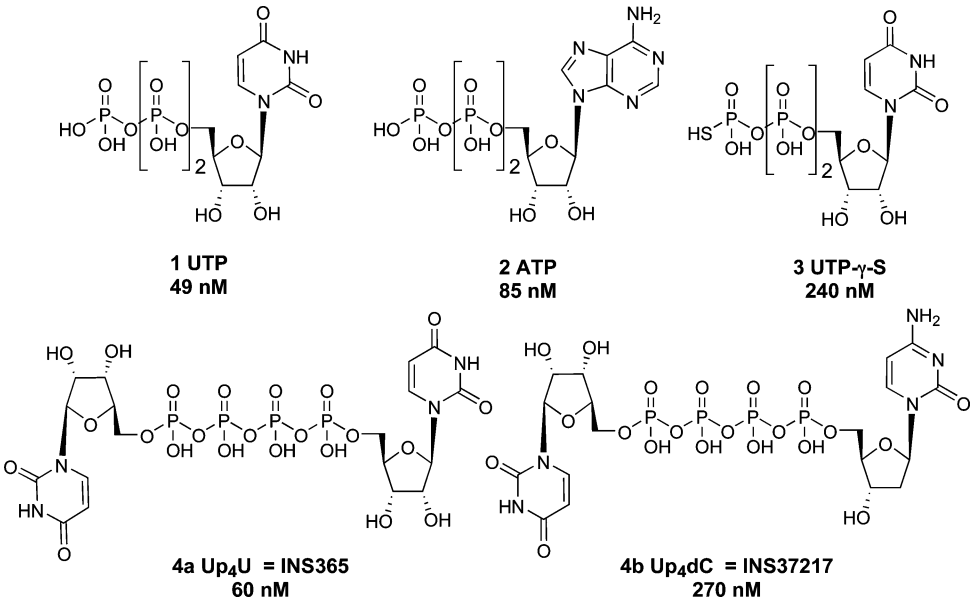

[a] EC_{50} values reported at the human $P2Y_2$ receptor are shown.[13,23,24,42]

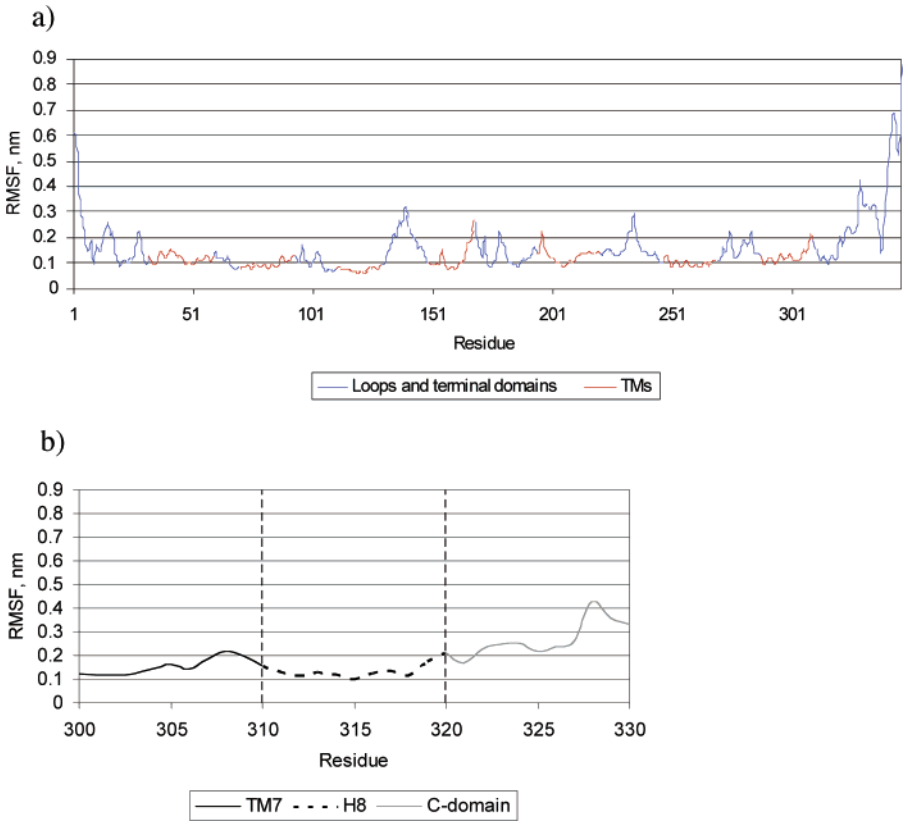

Figure 1. (a) The rmsf of the $P2Y_2$ receptor residues calculated from the 10 ns MD trajectory. (b) The rmsf of a part of the C-terminal region of the $P2Y_2$ receptor. A helical structure of H8 remained stable during the MD simulation.

Inclusion of the natural environment of the receptor was previously shown to significantly improve the results of MD simulation, providing a more accurate structure of the receptor, especially in its loop and terminal regions.[17] Therefore, the model was subjected to 10 ns of MD simulation in a hydrated phospholipid bilayer.

The MD trajectory was analyzed, and the root-mean-square deviations (rmsd) of the $P2Y_2$ receptor atoms, as well as its total energy, were calculated (Supporting Information). The analysis of the variation of the rmsd and the total energy along the trajectory suggested that during MD simulation the receptor structure became stable after 7.5 ns. Thus, we prolonged the simulation up to 10 ns and used the final typical structure for our docking studies. Also, the rms fluctuations (rmsf) of the $P2Y_2$ receptor residues were calculated from the MD trajectory. As shown in Figure 1, the lowest rmsf values were obtained for amino acid residues located in TM domains and the highest values corresponded to residues located in the hydrophilic loops

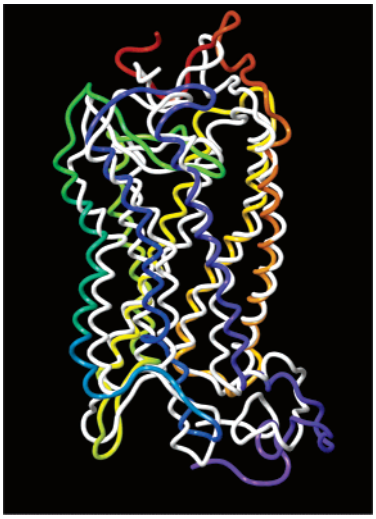

Figure 2. Superimposition of the initial structure of the human $P2Y_2$ receptor (white) and its structure obtained after MD simulation (colored by residue position: N-terminus in red, TM 1 in orange, TM 2 in ochre, TM 3 in yellow, TM 4 in green, TM 5 in cyan, TM 6 in blue, TM 7 and C-terminus in purple). Lipid and water molecules are not shown.

Table 1. Predicted Electrostatic and Disulfide Bridges Observed in the $P2Y_2$ Receptor Model Obtained after MD Simulation

residue	residue
Electrostatic Bridges	
negatively charged	positively charged
Glu20 NT	Arg26 NT
Glu20 NT	Arg177 EL2
Glu29 NT	Arg180 EL2
Asp30 NT	Arg24 NT
Asp97 EL1	Arg24 NT
Asp185 EL2	Arg 265 6.55
Glu190 EL2	Arg194 EL2
Asp319 CT	Arg340 CT
Asp342 CT	Arg334 CT
Asp345 CT	Arg335 CT
Disulfide Bridges	
Cys25 NT	Cys278 EL3
Cys106 3.25	Cys183 EL2
Putative Disulfide Bridges	
Cys132 3.51	Cys217 5.57
Cys44 1.43	Cys300 7.47

and terminal domains. The superimposition of the C_α atoms of the TM domains of the initial structure of the $P2Y_2$ receptor and its typical structure calculated from the final 100 ps of the MD trajectory (Figure 2) demonstrated that the configuration of the loops and terminal domains was most significantly changed.

1.1. Extracellular Regions. Recent MD simulation of the $P2Y_6$ receptor revealed that EL2 moved toward TM 3 and further up into the extracellular space, opening the putative nucleotide binding cavity.[18] However, in the case of the $P2Y_2$ receptor, EL2 did not show a significant displacement during the MD simulation. The analysis of the configuration of EL2 in the $P2Y_2$ receptor structure obtained after MD simulation allowed us to propose several key residues that could fix this loop near the TM domain (Table 1). In addition to the disulfide bridge conserved among all GPCRs of the rhodopsin family and formed between two cysteine residues located in TM 3 and EL2 (C106 and C183 in the $P2Y_2$ receptor), we found that several charged residues located in EL2 of the $P2Y_2$ receptor can interact with some oppositely charged residues located around the loop (Figure 3A). In particular, three pairs of such residues were observed: R177(EL2)−E20(NT), R180(EL2)−E29(NT), and D185(EL2)−R265(6.55). Throughout this paper we use the GPCR residue indexing system for TM regions, which allows comparison among receptors, as explained in detail elsewhere.[17] In addition, E190 can interact with R194; both residues are located at the beginning of EL2. Several other bridges in the extracellular region of the $P2Y_2$ receptor appeared in the model. R24(NT) can interact with D97(EL1) and with D30 (NT). Furthermore, E20(NT) interacted not only with R177-(EL2) but also with R26(NT). Finally, C25, located in the NT domain, and C278, located in EL3, formed a disulfide bridge characteristic of all P2Y receptors.

1.2. Intracellular Regions. Three possible pairs of charged residues were found in the intracellular region of the $P2Y_2$ receptor: D319−R340, R334−D342, and R335−D345 (Figure 3B). All these residues are located in the CT domain. Our molecular model suggests that ionic interactions between these residues keep the long CT domain in a more compact and configurationally restricted form, giving the entire receptor a more densely packed structure.

The rmsf values obtained for the residues located in the H8 helix (Figure 1b) showed that this part of the receptor remained stable during MD simulation, and H8 was found to be helical in the typical structure of the $P2Y_2$ receptor.

1.3. Putative Interhelical Disulfide Bridges. An analysis of the model obtained after MD simulation allowed us to hypothesize that two pairs of cysteine residues, C132(3.51)−C217(5.57) and C44(1.43)−C300(7.47), can be involved in the formation of disulfide bridges (Figure 3B). The distances observed between C_β atoms of these cysteines (6.2 and 4.5 Å, respectively) are in good agreement with the distances measured experimentally for disulfide-bonded Cys−Cys pairs.[19] However, C1.43 and C3.51 are present in the $P2Y_2$ receptor only; in other subtypes of P2Y receptors these residues are F1.43 and Y3.51 (except F3.51 in the $P2Y_{13}$). For this reason, these two proposed disulfide bridges could only exist in the $P2Y_2$ receptor. It has been shown experimentally that in rhodopsin the formation of a disulfide bond between residues located at the 3.51 and 5.57 positions is possible and that a cross-link between Y3.51C and C5.57 inhibits rhodopsin activation.[20]

2. Putative Binding Modes of $P2Y_2$ Receptor Agonists. 2.1. Binding Mode of UTP and Its Analogues. To study the putative binding modes of $P2Y_2$ receptor agonists, we performed molecular docking combined with the Monte Carlo multiple minimum (MCMM) conformational search analysis on several known nucleotide ligands of this receptor subtype. As described in the Experimental Section, UTP **1** initially was manually docked inside the putative binding site of the $P2Y_2$ receptor. The published data of site-directed mutagenesis combined with computational studies of P2Y receptors were taken into account.[1,13,18] Because the Northern (N) conformation of the ribose ring of the ligand was proposed to be important for recognition,[21] UTP and all other studied ligands were sketched and initially docked in their (N)-conformation. In addition, the anti conformation of the ligand base ring was used during the modeling studies. Interestingly, in the original rhodopsin-based model of the $P2Y_2$ receptor,[1] the side chain of one of the key cationic residues, namely R3.29, was oriented in the opposite direction from the putative binding pocket, but during the simulation it shifted toward the binding cavity.

After MCMM refinement of the initially obtained docking complex, the α-phosphate group of the UTP triphosphate chain was bonded to R7.39 whereas R6.55 could interact with both α- and γ-phosphate groups and R3.29 interacted with the γ-phosphate group of UTP (Figure 4A). In addition, the

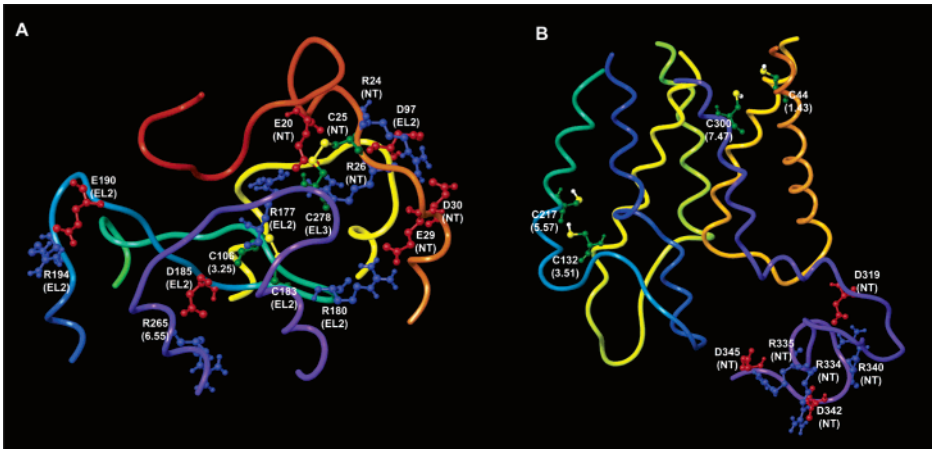

Figure 3. Putative electrostatic and disulfide bridges found in the extracellular (A) and intracellular (B) regions of the model of the $P2Y_2$ receptor.

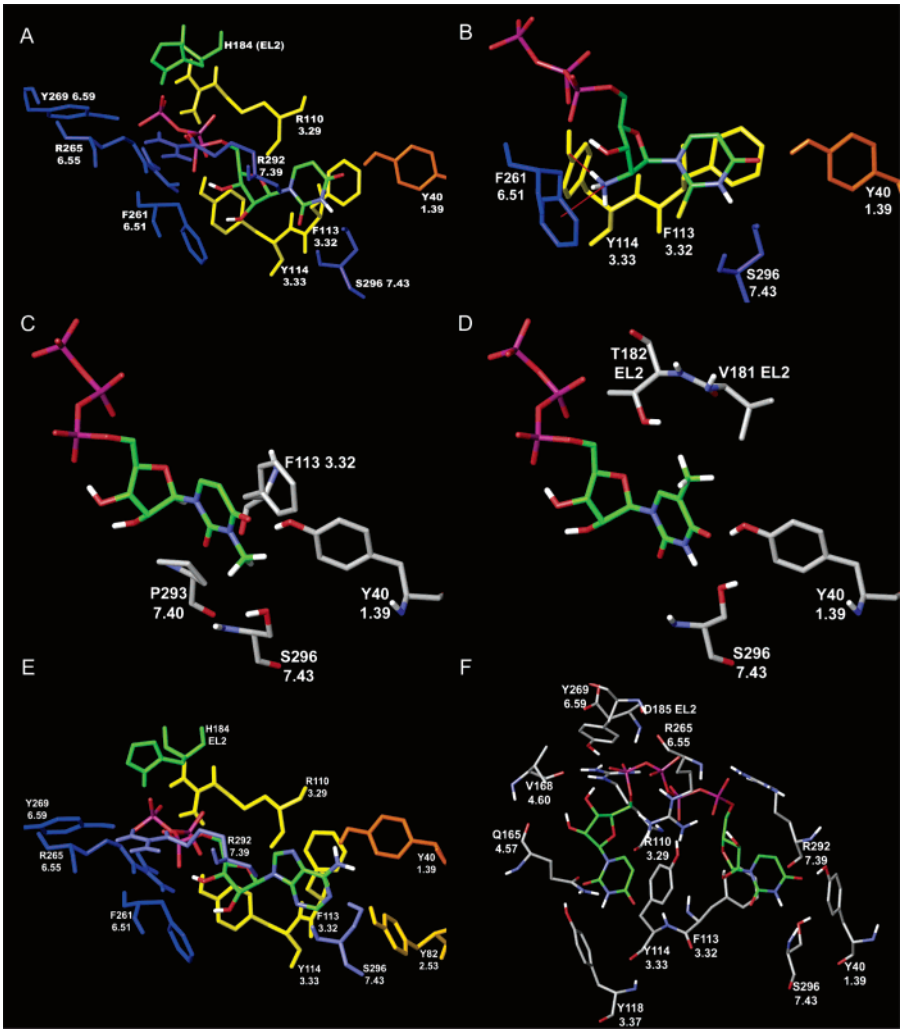

Figure 4. Binding modes of various agonists to the human $P2Y_2$ receptor following MCMM calculations: (A) UTP **1**; (B) 2′-amino-2′-deoxy analogue **8** of UTP, where the 2′-amino group is shown in its protonated form, which can be involved in cation$-\pi$ interactions with F6.51 and can form an additional H-bond with Y3.33; (C) 3-methyl-UTP,[13] where the 3-methyl group has an unfavorable position between hydroxyl groups of Y1.39 and S7.43, and backbone oxygen atom of P7.40; (D) 5-methyl-UTP **19**,[13] where, in the model obtained, the 5-methyl group of **19** is unfavorably located between hydroxyl groups of T182 (EL2) and Y1.39 and is close to the methyl groups of V181 (EL2); (E) ATP **2**; (F) Up_4U **4a**.

γ-phosphate group of the ligand formed H-bonds with H184, located in EL2 directly after the conserved cysteine residue, with the backbone nitrogen atom of D185 and with the hydroxyl group of Y6.59. Another tyrosine residue, Y3.33, was H-bonded to the β-phosphate group.

In the model obtained after MCMM calculations, the 2′-hydroxyl group of UTP appeared near the conserved F6.51 (in the $P2Y_{11}$ and $P2Y_{14}$ receptors, this position is Y6.51). This observation suggests the possibility of OH$-\pi$ H-bonding between the 2′-hydroxyl group and the aromatic ring of F6.51. Several examples of similar interactions seen in protein crystallographic structures were reviewed by Meyer et al.[22] The hypothesis of H-bonding of the 2′-hydroxyl group to the receptor is consistent with the experimental SAR.[13] For example, 2′-

Table 2. In Vitro Pharmacological Data for UTP **1** and Its Analogues in the Stimulation of PLC at Recombinant Human $P2Y_2$, $P2Y_4$, and $P2Y_6$ Receptors Expressed in 1321N1 Astrocytoma Cells (Unless Otherwise Noted, R^1 = OH, X = O, and R^2 = H)

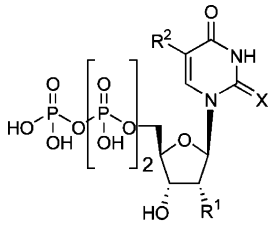

1, 6 – 10, 17 – 19

			EC_{50},[a] nM		
compd	modification	structure	at $hP2Y_2$ receptor	at $hP2Y_4$ receptor	at $hP2Y_6$ receptor
1[b]	(=UTP)		49 ± 12	73 ± 20	>10000[e]
2[b]	(=ATP)		85 ± 12	antagonist[d]	NE[g]
4a	(=Up_4U)		210 ± 30	130 ± 10	20000[e]
5	(=Up_4[5]ribose)		1880 ± 30	ND[h]	ND[h]
6[b]	2′-deoxy−2′-amino	$R^1 = NH_2$	62 ± 8	1200 ± 300	>100000
7[b]	2-thio	X = S	35 ± 4	350 ± 10	~1500[f]
8[c]	2-thio-2′-deoxy−2′-amino	X = S, $R^1 = NH_2$	8 ± 2	2400 ± 800	>10000
9	2-thio-2′-deoxy−2′-trifluoroacetylamino	X = S, $R^1 = CF_3CONH$	470 ± 60	8300 ± 1200	NE[g]
10	2-thio-2′-deoxy−2′-acetylamino	X = S, $R^1 = CH_3CONH$	6500 ± 1400	NE[g]	NE[g]
17	5-amino	$R^2 = NH_2$	5600 ± 1200	ND[h]	333 ± 88
18	5-azido	$R^2 = N_3$	1800 ± 400	ND[h]	467 ± 120
19[b]	5-methyl	$R^2 = CH_3$	480 ± 100	3900 ± 1600	140 ± 30

[a] Agonist potencies reflect stimulation of PLC determined as reported,[13,21,30] unless otherwise noted, and were calculated using a four-parameter logistic equation and the GraphPad software package (GraphPad, San Diego, CA). EC_{50} values (mean ± standard error) represent the concentration at which 50% of the maximal effect is achieved. The potency of UDP at the $P2Y_6$ receptor was 23 ± 4 nM. $N = 3$. [b] Agonist potencies from ref 13. [c] MRS2698. [d] ATP antagonized the human $P2Y_4$ receptor with a K_B of 708 nM. [e] Agonist potencies in mobilization of intracellular [Ca^{2+}], from refs 23 and 24. [f] Agonist potency from ref 26. [g] NE: no effect at 10 μM. [h] ND: not determined.

deoxy-UTP (EC_{50} = 1.08 μM) is 22-fold less potent than UTP (EC_{50} = 0.049 μM), whereas the replacement of the 2′-hydroxyl group by a 2′-methoxy group (EC_{50} = 14.3 μM) reduced the potency further (290-fold weaker than UTP). In the latter case, our model showed that not only was the suggested OH−π H-bond lost but the 2′-methyl group also interfered sterically with the aromatic ring of F6.51.

Agonist activities of the ligands, taken together with the binding mode obtained, strongly suggest that the hydroxyl group at the 2′ position is important as a donor but not as an acceptor of a H-bond. The binding mode of 2′-deoxy-2′-amino-UTP **6** (Table 2, EC_{50} = 0.062 μM), which was found to maintain potency in activation of the $P2Y_2$ receptor,[13] was studied with MCMM calculations. The 2′-amino group (pK_a = 6.2 in a related derivative)[40,41] was examined in both unprotonated and protonated positively charged forms. Similar to the 2′-hydroxyl group of UTP, the 2′-amino group of **6** was found near and oriented toward the aromatic ring of F6.51. Both protonated and unprotonated forms of the ligands interacted with this residue. However, the protonated form of this amino group was involved in a stronger cation−π interaction with F6.51. In addition, the protonated 2′-NH_3^+ group acted as a H-bond donor to the hydroxyl of Y3.33 in our model (Figure 4B).

In the receptor−ligand complexes obtained for all studied agonists, the 3′-hydroxyl group of the ligand appeared to be H-bonded to the α-phosphate group of the triphosphate chain. This could be an important intramolecular interaction to stabilize the ribose ring in its (N)-conformation, to facilitate the interaction of the 2′-hydroxyl group with F6.51. This assumption is in agreement with the ligand activities;[13,21] both 3′-deoxy-3′-methoxy-UTP and (S)-methanocarba ATP are essentially inactive at the $P2Y_2$ receptor.

Taken together, these findings are in good agreement with the SAR data and can explain the experimentally observed differences in activities of UTP and its 3′- and 2′-substituted derivatives: UTP ~ 2′-NH_2-2′-dUTP > 2′-dUTP > 2′-OCH_3-2′-dUTP ≫ 3′-OCH_3-3′-dUTP.

In our model the oxygen atom at position 4 of the UTP uracil ring was H-bonded to the hydroxyl group of Y1.39, and S7.43 accepted a H-bond from the 3-NH group of the ligand. In contrast, the oxygen atom at position 2 was not involved in H-bonding with the receptor. In addition, F3.32, conserved among all subtypes of P2Y receptors, was found to be involved in $\pi-\pi$ interaction with the uracil ring of UTP. Interestingly, in the model obtained for the complex of the $P2Y_2$ receptor with CTP (EC_{50} = 5.63 μM),[13] the hydroxyl group of S7.43 was involved in H-bonding with the nitrogen atom at the 3 position of the nucleobase of CTP, but the NH_2 group at the 4 position was unable to form a H-bond with Y1.39. Furthermore, the nucleoside moiety of zebularine 5′-triphosphate (180-fold weaker than UTP)[13] docked to the $P2Y_2$ receptor was significantly shifted from the initial position of UTP outwardly and toward Y1.39, although the ligand still maintained a H-bond with S7.43. In addition, it was shown that a thiouracil ring can form H-bonded pairs with other nucleobases, which are only slightly less stable than the pairs formed by unmodified uracil.[39] This means that 4-thio-UTP could be involved in the same interactions with Y1.39 as UTP. These data argue in favor of the hypothesis that in the case of the $P2Y_2$ receptor, Y1.39 plays a role in the recognition of the functional group at position 4 of the uracil moiety. Available experimental data indicate that 3-methyl-UTP (EC_{50} = 1.20 μM) is 24-fold weaker than UTP.[13] With the aim of explaining the observed differences in activity, we used MCMM calculations to establish a favored binding mode of 3-methyl-UTP, which was compared to the binding mode of UTP. According to this model, the methyl group at position 3 was located between the hydroxyl groups of Y1.39 and S7.43, and the side chain of the serine residue was shifted

Scheme 1. Preparation of the Synthetic Intermediate **15**, a 2′-Amino-2′-deoxy-2-thio Nucleoside[a]

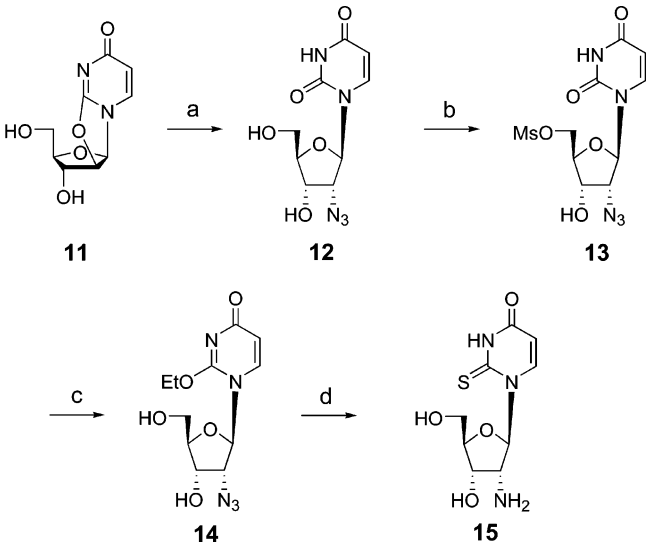

[a] Reagents and conditions: (a) NaN_3, DMF, 150 °C, 15 h; (b) MsCl, pyridine, 0 °C, 61%; (c) $NaHCO_3$/EtOH, reflux, 36 h, 57%; (d) H_2S, pyridine, 50 °C, 250 psi, 24 h, 77%.

by 1.5 Å away from the ligand. Moreover, the backbone oxygen atom of P7.40 also appeared near the 3-methyl group (Figure 4C).

The binding modes of 5-bromo- ($EC_{50} = 0.75\ \mu M$), 5-iodo- ($EC_{50} = 0.83\ \mu M$), and 5-methyl-UTP ($EC_{50} = 0.48\ \mu M$) were determined (Figure 4D) indicating that a hydrophobic group at position 5 of UTP was located unfavorably between the hydrophilic hydroxyl groups of T182 (EL2) and Y1.39. The methyl groups of V181 (EL2) were also located approximately 4 Å from the substituent at position 5. Therefore, our model suggested that the introduction of a small hydrophilic group, such as an amino or hydroxyl group, at position 5 could provide additional H-bonds with T182 and Y1.39 and thus favor potency. Also, we predicted that an azido group would interact favorably within the available space between Y40, R180, V181, T182, and P293.

2.2. Binding Mode of ATP. The question of whether UTP and ATP bind to the same site in the $P2Y_2$ receptor has already been considered.[3] Because ATP **2** ($EC_{50} = 0.085\ \mu M$) and UTP **1** ($EC_{50} = 0.049\ \mu M$) are nearly equipotent at the $P2Y_2$ receptor, ATP was initially docked (Figure 4E) at the $P2Y_2$ receptor with the ribose in the (N)-conformation and the adenine ring in the anti conformation and subsequently subjected to an MCMM conformational search. Superimposition of the ATP−$P2Y_2$ and the UTP−$P2Y_2$ complexes revealed that the phosphate chains and the ribose rings of these two ligands have identical positions and configurations inside the receptor. The residues interacting with UTP were also found to interact with ATP. In agreement with the binding mode obtained for UTP, F3.32 was involved in a $\pi-\pi$ interaction with the adenine ring of ATP. Also, Y1.39 was H-bonded with the N^6-amino group, whereas S7.43 was H-bonded with the nitrogen atom at position 1 of the adenine ring of ATP. In addition, Y2.53, conserved among $P2Y_{1,2,4,6}$ receptors, formed a H-bond with the nitrogen atom at position 1. On this basis, we propose that Y2.53 is likely more important for interactions of the $P2Y_2$ receptor with ATP and its derivatives than with UTP analogues.

2.3. Binding Mode of Dinucleotide Agonists. The $P2Y_2$ receptor can be activated not only by uracil or adenine triphosphates but also by dinucleotide molecules.[23,24] Dinucleotide tetraphosphates, such as Up_4U **4a** or Up_4dC **4b** (Chart 1), have the optimal phosphate chain length for activation of the $P2Y_2$ receptor and tend to be more resistant to nucleotidase degradation than the nucleoside triphosphates. In contrast, Up_2U, containing only two phosphate groups, is nearly inactive as an agonist, and Up_6U is 98-fold weaker than Up_4U at the $P2Y_2$ receptor.

To study the binding mode of dinucleotides within the $P2Y_2$ receptor, we docked Up_4U to the putative binding site. Docking of molecules that are as complex as Up_4U is challenging because of their large size and great flexibility. In particular, this process is especially difficult in the absence of X-ray structures or even molecular models of the receptor complexed with similar ligands. Several methods for docking of large ligands were described previously.[25] In particular, fragmental-guided docking methods decompose a ligand into small fragments and then use favorable binding modes of these fragments to determine the most favorable orientation of the whole ligand.

Here, we introduce an alternative "sequential ligand composition" technique, which we applied to the molecular docking of Up_4U. With this technique, the structure of UTP docked in the binding site of the $P2Y_2$ receptor and subjected to MCMM calculations was sequentially converted to Up_4, Up_4-ribose, and Up_4U. The MCMM conformational search analysis of the ligand and all receptor residues located within 5 Å of the ligand was performed at each stage of the computational conversion of UTP to Up_4U to provide an energetically favorable orientation and configuration of the ligand. In contrast to the docking of the entire structure of the ligand (e.g., Up_4U) at once, this method can avoid undesirable changes in the configuration of the receptor binding site.

Thus, "sequential ligand composition" provided us with a putative binding mode of Up_4U at the $P2Y_2$ receptor (Figure 4F and Supporting Information). In our model, the common uridine triphosphate subset of the Up_4U structure had almost the same binding mode as UTP. However, three residues that interacted with the γ-phosphate group of UTP, i.e., R3.29, D185 (EL2), and Y6.59, were found to be bonded to the δ-phosphate group of Up_4U. The uracil ring of UTP ($uracil^{I}$) was involved in a $\pi-\pi$ interaction with F3.32, and the uracil ring of the second uridine moiety ($uracil^{II}$) of Up_4U formed $\pi-\pi$ interactions with Y3.33, which was also bonded to the β-phosphate group of the ligand. The oxygen atom at the 2 position of the $uracil^{II}$ ring could form H-bonds with Q4.57 and Y3.37. The oxygen atom of the hydroxyl group of Y3.37 also appeared near the 3-NH $group^{II}$ of the ligand and could be involved in H-bonding with this group. As was observed with UTP, neither of the ribose ring oxygen atoms was H-bonded to the receptor. However, the 3′-hydroxyl groups of both $uridine^{I}$ and $uridine^{II}$ of Up_4U were H-bonded to the α and δ phosphate groups, respectively.

The model of receptor-docked Up_4U is consistent with a tetraphosphate chain having the optimal length for dinucleotide binding. The phosphate side chain of diuridine diphosphates apparently is too short to allow $uridine^{II}$ to reach its binding pocket. In contrast, ligands with longer phosphate chains, such as Up_6U, are too large to be fully accommodated inside the receptor. Also, as discussed by Brunschweiger and Müller,[2] among various linear dinucleotides only dinucleoside tetraphosphates have the same number of negatively charged oxygen atoms as UTP.

Although H-bonds between the $P2Y_2$ receptor and the ribose ring oxygen of $uridine^{II}$ of Up_4U are absent, both 2′- and 3′-hydroxyl groups were found to be H-bonded to the receptor.

Scheme 2. Synthesis of 2′-Amino-2′-deoxy-2-thio-UTP **8** and Its *N*-Trifluoroacetyl Derivative **9**[a]

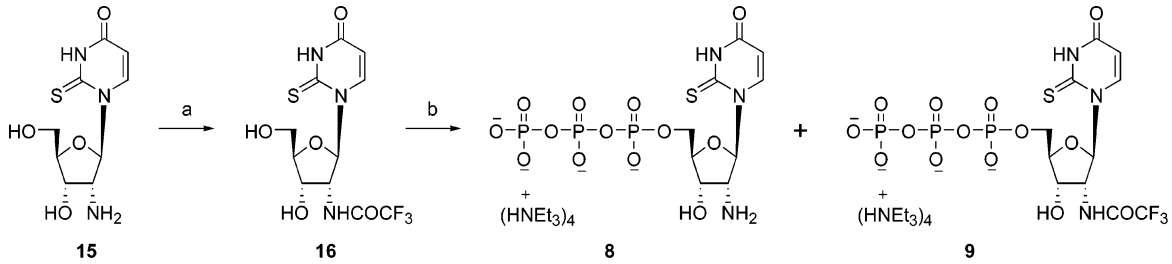

15 16 8 9

[a] Reagents and conditions: (a) DIEA, ethyl trifluoroacetate, DMF, room temperature, 13 h, 88%; (b) (i) $POCl_3$, $PO(OCH_3)_3$, Proton Sponge, 0 °C, 2 h; (ii) $(Bu_3NH^+)_2P_2O_7H_2$, Bu_3N, DMF, 10 min; (iii) 0.2 M triethylammonium bicarbonate solution, room temperature, 1 h, 12% (**8**), 7% (**9**).

The 2′-hydroxyl group was found to be H-bonded with the hydroxyl group of Y5.38, and the 3′-hydroxyl group interacted with the backbone NH group of V4.60. Also, the hydroxyl group of Y6.59 appeared near the 3′-hydroxyl group of the ligand. These observations suggest that Up_4-ribose could be active at the $P2Y_2$ receptor, as UDP-glucose is active at the $P2Y_{14}$ receptor. In the complex obtained for Up_4U, both the hydroxyl group of Tyr and the backbone NH group of Val were found 5.5 Å from the ligand.

2.4. Selective Recognition for Nucleoside Tri- and Diphosphates at $P2Y_2$ and $P2Y_6$ Receptors. Although UDP is almost inactive at the $P2Y_2$ receptor,[2] it is the cognate agonist of the $P2Y_6$ receptor. Although UTP analogues may display considerable potency at the $P2Y_6$ receptor,[26] UTP itself is nearly inactive. To explain these differences, we compared residues of the $P2Y_2$ receptor directly involved in ligand interactions with the corresponding residues of the $P2Y_6$ receptor (details are given in Supporting Information). The results obtained allow us to propose that residues R/K6.55, Y/L6.59, and H184/Y178 of the $P2Y_2$/$P2Y_6$ receptors play a critical role in UTP versus UDP recognition. This hypothesis will be tested in future experiments with site-directed mutagenesis.

3. Exploration of SAR at the $P2Y_2$ Receptor with the Aid of Modeling. To further examine determinants of $P2Y_2$ receptor selectivity, we synthesized several nucleotide derivatives and tested them for activation of the human $P2Y_2$ and $P2Y_4$ receptors expressed in 1321N1 astrocytoma cells (Table 2). The 2′-amino modification of **6**, which maintained potency at the $P2Y_2$ receptor,[13] was combined with another $P2Y_2$-favorable modification of UTP, i.e., 2-thio, leading to **8**. The requirement of a free amine at this position was explored through N-acylation reactions, leading to **9** and **10**. Although a 5-methyl modification of the uracil ring of UTP was found to reduce $P2Y_2$ receptor potency,[13] we also examined whether introduction of a polar, H-bonding group such as amino at this position would be beneficial. Thus, the 5-amino **17** and 5-azido **18** analogues were evaluated at the receptors.

3.1. Chemical Synthesis. 2′-Amino-2′-deoxy-2-thiouridine 5′-triphosphate **8** was prepared by standard phosphorylation of the corresponding nucleoside **15**. The synthesis of 2′-amino-2′-deoxy-2-thiouridine **15** is depicted in Scheme 1. 2′-Azido-2′-deoxyuridine **12** was obtained via opening of 2,2′-anhydrouridine with NaN_3 in DMF.[27] After selective mesylation of the 5′-hydroxyl group of **12**, the resulting 5′-methanesulfonate ester **13** was converted to 2′-azido-2′-deoxy-2-*O*-ethyluridine (**14**) according to the method of Manoharan and co-workers.[28] In this reaction, 2,5′-anhydro-2′-azido-2′-deoxyuridine was generated in situ and subsequently opened with ethoxide. Treatment of **14** with H_2S in anhydrous pyridine allowed simultaneous 2-thionation and reduction of the 2′-azido group, resulting in 2′-amino-2′-deoxy-2-thiouridine (**15**). The 2-thionation was confirmed by the ^{13}C NMR resonance signal of C-2, which shifts to a low magnetic field (177.66 ppm) compared to uridine (150.66 ppm).

Scheme 3. Synthesis of 2′-Acetylamino-2′-deoxy-2-thio-UTP **10**[a]

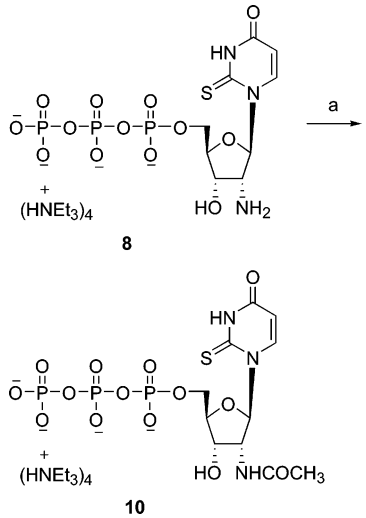

8 10

[a] Reagents and conditions: (a) acetic anhydride, H_2O, room temperature, 6 h, 57%.

Scheme 4. Synthesis of Up_4-5′-ribose **5**[a]

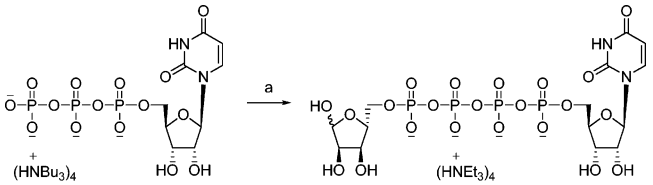

1 5

[a] Reagents and conditions: (a) (i) DCC, DMF, room temperature, 1 h; (ii) D-ribose 5-phosphate, DMF, room temperature, 48 h, 18%.

Attempts to directly phosphorylate compound **15** by a standard method failed to yield the desired 5′-triphosphate **8**. Therefore, the 2′-amino group was protected by trifluoroacetylation. The phosphorylation of the protected nucleoside **16** was performed as shown in Scheme 2.[29] During purification by ion exchange chromatography, partial hydrolysis yielded a mixture of **8** and **9**, which was readily separable by HPLC. The acetylation of the 2′-amino group of **8** to obtain **10** was performed as shown in Scheme 3. Up_4ribose **5** was prepared as shown in Scheme 4.

3.2. Pharmacological Activity. Activation of PLC by a range of concentrations of each nucleotide derivatives was studied in 1321N1 astrocytoma cells stably expressing the human $P2Y_2$, $P2Y_4$, and $P2Y_6$ receptors (Table 2), by reported methods.[13,21,30,31] Tritiated inositol phosphates produced from a radiolabeled myo-inositol precursor were measured using a standard ion exchange method.

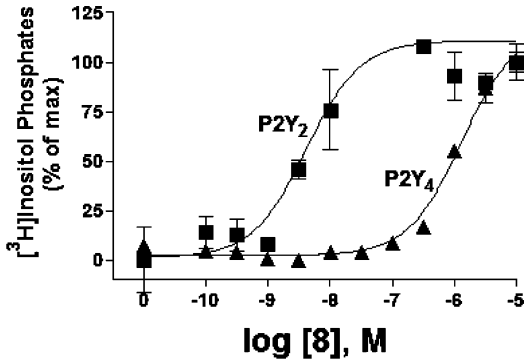

Figure 5. Activation by compound **8** of PLC in 1321N1 astrocytoma cells expressing the human $P2Y_2$ receptor or $P2Y_4$ receptor.

An intermediate structure related to the modeling by "sequential ligand composition", Up_4-[5′]-ribose **5**, activated the $P2Y_2$ receptor with an EC_{50} of 1.88 μM, i.e., 9-fold less potent than Up_4U.

The 5′-triphosphate **8**, which combined potency-enhancing features derived from our previous studies, was 300-fold selective in activation of the $P2Y_2$ receptor in comparison with the $P2Y_4$ receptor (Figure 5). Compound **8** and other 2′-deoxy-2′-amino analogues, **6**, **9**, and **10**, were nearly inactive at the $P2Y_6$ receptor. The binding mode of this potent and selective analogue was studied with MCMM calculations, and the results were similar to those for **6**, in which the 2′-amino group in its protonated form was involved in a cation$-\pi$ interaction with F6.51 and as a H-bond donor to Y3.33 (Figure 4B). The potency of **8** was greatly reduced upon acetylation (**10**) and reduced to a lesser degree upon trifluoroacetylation (**9**). These observations are consistent with the binding modes obtained for compound **10**. In the model of the $P2Y_2$ receptor complex with compound **10** (Supporting Information), the H-bond between F6.51 and the NH group of the acetamide moiety was not observed. Moreover, the methyl group of this moiety undesirably appeared near the OH group of Y3.33 and the NH_2 group of R6.55. The oxygen atom of the acetyl group was not involved in interactions with the receptor. We speculate that in the case of compound **9**, the CF_3 group, which is more electronegative than CH_3, provides some favorable interactions with positively charged R6.55, improving the potency of compound **10**.

The 5 position was predicted to accommodate an azido group as well as a small, polar, H-bonding group, such as an amino group. Building on these observations, we measured the activities of 5-amino **17** and 5-azido **18** UTP derivatives at the human $P2Y_2$ receptor (Table 2). However, the results indicated that both structures are less active than 5-methyl-UTP **19** at this receptor.[13] Similar to certain other uracil-substituted uridine 5′-triphosphates,[26] compounds **17**−**19** also potently activated the human $P2Y_6$ receptor.

Introduction of an amino or azido group at position 5 of UTP apparently influences the conformation of the ribose ring. It was shown previously,[32] through NMR analysis combined with semiempirical calculations, that electron-donating groups at position 5 of uracil nucleotides can destabilize the $P2Y_2$ receptor-preferred (N)-conformation of the ribose ring.

Conclusions

This detailed view of molecular recognition at the $P2Y_2$ receptor suggests mutations for further model validation. In this study we report a highly potent and selective agonist, the 2′-amino-2-thio derivative of UTP, compound **8**, which should prove to be very useful as a pharmacological probe for studying $P2Y_2$ receptor action. Modeling provided an explanation for the general stabilizing effect of the 2′-amino modification of UTP in $P2Y_2$ receptor recognition. A "sequential ligand composition" approach was adopted for docking flexible dinucleotide agonists such as Up_4U. This modeling approach, in which ligands are docked to the receptor (including loops and terminal regions), embedded in a phospholipid bilayer, and optimized with MCMM, promises to be helpful in the design of additional potent and selective $P2Y_2$ receptor agonists.

Experimental Section

Chemical Synthesis. All reagents were from standard commercial sources and of analytic grade. Compounds **17** and **18** were purchased from ALT, Inc. (Lexington, KY). 2,2′-Anhydrouridine (**11**) was obtained from Wako Chemicals GmbH (Neuss, Germany). Precoated Merck silica gel F254 plates were used for TLC, and spots were examined under ultraviolet light at 254 nm and further visualized by sulfuric acid−anisaldehyde spray. Column chromatography was performed on ICN silica gel (63−200 μm, 60 Å, ICN Biochemicals, Eschwege, Germany). For compounds **11**−**15**, NMR spectra were obtained with a Varian Mercury 300 MHz spectrometer. Chemical shifts are given in ppm (δ) relative to the residual solvent signal; in the case of DMSO-d_6, the shift is 2.54 ppm for ^{1}H and 40.5 ppm for ^{13}C. Structural assignment was confirmed with correlation spectroscopy (COSY) and distortionless enhancement by polarization transfer (DEPT) experiments. All signals assigned to hydroxyl groups were exchangeable with D_2O. Exact mass measurements were performed on a quadruple orthogonal-acceleration time-of-flight (Q/oaTOF) tandem mass spectrometer (qToF 2, Micromass, Manchester, U.K.) equipped with a standard electrospray ionization (ESI) interface. Samples were infused in a 2-propanol/water (1:1) mixture at 3 μL/min. For compounds **16** and **8**−**10**, ^{1}H NMR spectra were obtained with a Varian Gemini 300 spectrometer (Varian, Inc., Palo Alto, CA). ^{31}P NMR spectra were recorded at room temperature with a Varian XL 300 spectrometer (121.42 MHz); orthophosphoric acid (85%) was used as an external standard. Purity of compounds was checked with a Hewlett−Packard 1100 HPLC equipped with a Zorbax Eclipse 5 μm XDB-C18 analytical column (250 mm × 4.6 mm; Agilent Technologies Inc., Palo Alto, CA). Purity was measured with two different solvent systems. (System A: 5 mM TBAP (tetrabutylammonium dihydrogen phosphate)/CH_3CN from 80:20 to 40:60 in 20 min; flow rate of 1 mL/min. System B: 10 mM TEAA (triethylammonium acetate)/CH_3CN from 80:20 to 60:40 in 20 min; flow rate of 1 mL/min. System C: 10 mM TEAA/CH_3CN from 100:0 to 80:20 in 20 min; flow rate of 1 mL/min.) Purifications by HPLC were performed under the following conditions: Luna 5 μm RP-C18 (2) semipreparative column, 250 mm × 10.0 mm, Phenomenex, Torrance, CA; flow rate of 2 mL/min. System D: 10 mM TEAA/CH_3CN from 100:0 to 90:10 in 20 min. System E: 10 mM TEAA/CH_3CN from 100:0 to 95:5 in 30 min. High-resolution mass measurements were performed on a Micromass/Waters LCT Premier electrospray time-of-flight mass spectrometer coupled with a Waters HPLC system (Waters Corp., Milford, MA).

2′-Azido-2′-deoxy-5′-*O*-methanesulfonyluridine (13). Methanesulfonyl chloride (210 μL, 2.7 mmol) was added to a solution of **12** (610 mg, 2.3 mmol) in 10 mL of pyridine at −78 °C. The mixture was stirred for 1 h at 0 °C, quenched with aqueous saturated $NaHCO_3$, extracted with CH_2Cl_2, dried over $MgSO_4$, filtered, and concentrated in vacuo. The residue was purified by column chromatography (CH_2Cl_2/MeOH, 96:4) to obtain compound **13** as a white solid (472 mg, 61%). ^{1}H NMR (DMSO-d_6): δ 3.23 (s, 3H, CH_3), 4.06 (m, 1H, H-4′), 4.25−4.48 (m, 4H, H-2′, H-3′, H-5′A, and H-5′B), 5.68 (dd, J = 7.9, 2.1 Hz, 1H, H-6), 5.82 (d, J = 5.3 Hz, 1H, 3′-OH), 6.2 (d, J = 5.6 Hz, 1H, H-1′), 7.62 (d, J = 8.2 Hz, 1H, H-5), 11.47 (s, 1H, NH). HRMS (ESI-MS) for $C_{10}H_{14}N_5O_7S$: $[M + H]^+$ found, 348.0618; calcd, 348.0613.

2′-Azido-2′-deoxy-2-*O*-ethyluridine (14). Compound **13** (465 mg, 1.3 mmol) was refluxed in absolute ethanol (60 mL) in the presence of anhydrous sodium bicarbonate (281 mg, 3.3 mmol)

under a nitrogen atmosphere for 36 h. After cooling to room temperature, the mixture was diluted with ethyl acetate and the precipitated sodium salt was removed by filtration. The filtrate was concentrated in vacuo and purified on a silica gel column (CH_2Cl_2/MeOH, 95:5) to obtain compound **14** (222 mg, 57%) as a white solid. ^{1}H NMR (DMSO-d_6): δ 1.33 (t, J = 6.9 Hz, 3H, CH_3), 3.56−3.63 (m, 1H, H-5′A), 3.67−3.74 (m, 1H, H-5′B), 3.92 (m, 1H, H-4′), 4.12 (app t, J = 4.8 Hz, 1H, H-3′), 4.27−4.39 (m, 3H, CH_2 and H-2′), 5.23 (t, J = 4.8 Hz, 1H, 5′-OH), 5.85 (m, 2H, H-6 and 3′-OH), 6.01 (d, J = 5.4 Hz, 1H, H-1′), 7.98 (d, J = 7.8 Hz, 1H, H-5). HRMS (ESI-MS) for $C_{11}H_{15}N_5O_5Na$: $[M + Na]^+$ found, 320.0974; calcd, 320.0971.

2′-Amino-2′-deoxy-2-thiouridine (15). In a Parr apparatus compound **14** (210 mg, 0.71 mmol) was dissolved in pyridine (40 mL), cooled to −50 °C, and saturated with H_2S. The mixture was heated at 50 °C for 24 h, resulting in a pressure of 250 psi. After the mixture was cooled to room temperature, the remaining H_2S was released, the solvent was evaporated, and the residue was purified on a silica gel column (CH_2Cl_2/MeOH, 90:10), yielding compound **15** (141 mg, 77%) after subsequent crystallization from MeOH. ^{1}H NMR (DMSO-d_6): δ 3.32 (dd, J = 6.1, 5.0 Hz, 1H, H-2′), 3.56−3.67 (m, 2H, H-5′A and H-5′B), 3.94 (m, 2H, H-3′ and H-4′), 5.19 (t, J = 4.7 Hz, 5′-OH), 5.41 (br s, 1H, 3′-OH), 6.01 (d, J = 8.2 Hz, 1H, H-6), 6.53 (d, J = 6.0 Hz, 1H, H-1′), 8.09 (d, J = 8.2 Hz, 1H, H-5). ^{13}C NMR (DMSO-d_6): δ 59.74 (C-2′), 61.43 (C-5′), 70.91 (C-3′), 86.50 (C-4′), 93.49 (C-1′), 107.32 (C-5), 141.66 (C-6), 160.24 (C-4), 177.66 (C-2). HRMS (ESI-MS) for $C_9H_{14}N_3O_4S_1$: $[M + H]^+$ found, 260.0692; calcd, 260.0704.

2′-Trifluoroacetylamino-2′-deoxy-2-thiouridine (16). *N*,*N*-Diisopropylethylamine (0.006 mL, 0.035 mmol) and ethyl trifluoroacetate (0.004 mL, 0.035 mmol) were added sequentially to a solution of **15** (6 mg, 0.023 mmol) in DMF (1 mL). The reaction mixture was stirred for 13 h at room temperature. The solvent was removed in vacuo, and the residue was purified by preparative thin-layer chromatography (CH_2Cl_2/MeOH, 90:10) to afford **16** (7.2 mg, 88%) as a white solid. ^{1}H NMR (CD_3OD): δ 3.84 (m, 2H, H-5′A and H-5′B), 4.14 (dd, J = 5.4, 2.7 Hz, 1H, H-4′), 4.34 (dd, J = 5.7, 3.0 Hz, 1H, H-3′), 4.58 (dd, J = 6.6, 6.3 Hz, 1H, H-2′), 6.01 (d, J = 8.1 Hz, 1H, H-6), 7.12 (d, J = 6.9 Hz, 1H, H-1′), 8.25 (d, J = 8.1 Hz, 1H, H-5). HRMS *m*/*z*: found 356.0520 $(M + H^+)^-$. $C_{11}H_{13}N_3O_5F_3S$ requires 356.0528.

2′-Amino-2′-deoxy-2-thiouridine 5′-Triphosphate Triethylammonium Salt (8) and 2′-Trifluoroacetylamino-2′-deoxy-2-thiouridine 5′-Triphosphate Triethylammonium Salt (9). Phosphorus oxychloride (0.004 mL, 0.04 mmol) was added to a solution of **16** (7.2 mg, 0.020 mmol) and Proton Sponge (4 mg, 0.033 mmol) in trimethyl phosphate (1 mL) at 0 °C. The reaction mixture was stirred for 2 h at 0 °C. Then a mixture of tributylamine (0.02 mL, 0.08 mmol) and tributylammonium pyrophosphate (1.6 mol of $C_{12}H_{27}N$ per mol of H_4PO_7, 62 mg, 0.131 mmol) in DMF (0.3 mL) was added at once. After 10 min, 0.2 M triethylammonium bicarbonate solution (2 mL) was added, and the clear solution was stirred at room temperature for 1 h. The latter was lyophilized overnight, and the resulting residue was purified by ion-exchange column chromatography with a Sephadex DEAE A-25 resin with a linear gradient (0.01−0.5 M) of 0.5 M ammonium bicarbonate as the mobile phase to get a mixture of **8** and **9** as the ammonium salts. The mixture was purified by HPLC (system D) to obtain **8** (2.2 mg, 12%) and **9** (1.4 mg, 7%) as the triethylammonium salts.

Compound 8. ^{1}H NMR (D_2O): δ 1.28 (t, J = 7.5 Hz, 36H, $N(CH_2CH_3)_3$), 3.20 (q, J = 7.5 Hz, 24H, $N(CH_2CH_3)_3$), 4.15 (dd, J = 6.9, 5.7 Hz, 1H, H-2′), 4.26 (m, 1H, H-5′A), 4.37 (m, 1H, H-5′B), 4.48 (m, 1H, H-4′), 4.86 (m, 1H, H-3′), 6.31 (d, J = 8.1 Hz, 1H, H-6), 7.22 (d, J = 7.2 Hz, 1H, H-1′), 8.12 (d, J = 8.1 Hz, 1H, H-5). ^{31}P NMR (D_2O): δ −22.64 (t, J = 20.2 Hz), −11.22 (d, J = 20.2 Hz), −9.63 (d, J = 19.6 Hz). HRMS *m*/*z*: found 497.9529 $(M - H^+)^-$. $C_9H_{15}N_3O_{13}P_3S$ requires 497.9538. Purity, >98% by HPLC (system A, 15.2 min; system B, 6.6 min).

Compound 9. ^{1}H NMR (D_2O): δ 1.28 (t, J = 7.5 Hz, 36H, $N(CH_2CH_3)_3$), 3.20 (q, J = 7.5 Hz, 24H, $N(CH_2CH_3)_3$), 4.32 (m, 2H, H-5′A and H-5′B), 4.58 (m, 1H, H-4′), 4.68 (m, 1H, H-2′), 4.80 (hidden by the water peak, 1H, H-3′), 6.26 (d, J = 8.1 Hz, 1H, H-6), 6.92 (d, J = 5.4 Hz, 1H, H-1′), 8.13 (d, J = 8.4 Hz, 1H, H-5). ^{31}P NMR (D_2O): δ −22.28 (t, J = 19.6 Hz), −11.04 (d, J = 19.6 Hz), −8.54 (m). HRMS *m*/*z*: found 593.9364 $(M - H^+)^-$. $C_{11}H_{14}N_3O_{14}P_3F_3S$ requires 593.9361. Purity, >98% by HPLC (system A, 18.3 min; system B, 7.7 min).

2′-Acetylamino-2′-deoxy-2-thiouridine 5′-Triphosphate Triethylammonium Salt (10). Acetic anhydride (0.07 mL, 0.74 mmol) was added to a solution of **8** (0.5 mg, 0.55 μmol) in H_2O (0.5 mL) at room temperature. After the reaction mixture was stirred for 6 h, the solvent was removed in vacuo. The residue was purified by HPLC (system D) to obtain **10** (0.3 mg, 57%) as the triethylammonium salts. ^{1}H NMR (D_2O): δ 1.28 (t, J = 7.5 Hz, 36H, $N(CH_2CH_3)_3$), 3.20 (q, J = 7.5 Hz, 24H, $N(CH_2CH_3)_3$), 4.29 (m, 2H, H-5′A and H-5′B), 4.36 (m, 1H, H-4′), 4.53 (m, 2H, H-2′ and H-3′), 6.27 (d, J = 8.1 Hz, 1H, H-6), 6.98 (d, J = 5.6 Hz, 1H, H-1′), 8.08 (d, J = 8.1 Hz, 1H, H-5). ^{31}P NMR (D_2O): δ −21.31 (t, J = 20.5 Hz), −10.84 (d, J = 20.8 Hz), −7.62 (m). HRMS *m*/*z*: found 539.9660 $(M - H^+)^-$. $C_{11}H_{17}N_3O_{14}P_3S$ requires 539.9644. Purity, >98% by HPLC (system A, 17.2 min; system B, 6.7 min).

Diuridine 5′,5′-Tetraphosphate Ammonium Salt (4a). Compound **4a** was synthesized by following the procedures of ref 23. HRMS *m*/*z*: found 788.9842 $(M - H^+)^-$. $C_{18}H_{25}N_4O_{23}P_4$ requires 788.9860. Purity, >98% by HPLC (system A, 20.5 min; system C, 7.7 min).

Uridine 5′-Tetraphosphate 5′-Ribose Triethylammonium Salt (5). Uridine 5′-triphosphate trisodium salt (25 mg, 0.05 mmol) and D-ribose 5-monophosphate disodium salt (59 mg, 0.19 mmol) were converted to the tributylammonium salts by treatment with the ion-exchange resin (DOWEX 50WX2-200 (H)) and tributylamine. After removal of the solvent, the resulting residue was dried under high vacuum overnight. To a solution of uridine 5′-triphosphate tributylammonium salt (0.05 mmol) in DMF (2 mL) was added *N*,*N*′-dicyclohexylcarbodiimide (22 mg, 0.11 mmol), and the mixture was stirred for 1 h at room temperature. A solution of d-ribose 5-monophosphate tributylammonium salt (0.19 mmol) in DMF (2 mL) was added to the reaction mixture, with stirring continuing at room temperature for 48 h. After removal of the solvent, the residue was purified by ion-exchange column chromatography with Sephadex DEAE A-25 resin using a linear gradient (0.01−0.5 M) of 0.5 M ammonium bicarbonate as the mobile phase. Compound **5** (7.0 mg, 18%) was additionally purified by HPLC (system E). ^{1}H NMR (D_2O): δ 1.28 (t, J = 7.5 Hz, 36H, $N(CH_2CH_3)_3$), 3.20 (q, J = 7.5 Hz, 24H, $N(CH_2CH_3)_3$), 4.11 (m, 3H, H-ribose), 4.28 (m, 4H, H-4′, H-5′, 1H-ribose), 4.42 (m, 3H, H-2′, H-3′, 1H-ribose), 5.22 (d, J = 2.4 Hz, 3/5H, H-1′ribose), 5.41 (d, J = 3.6 Hz, 2/5H, H-1′ribose), 5.99 (d, J = 8.3 Hz, 1H, H-5), 6.02 (d, J = 5.4 Hz, 1H, H-1′), 7.99 (d, J = 8.3 Hz, 1H, H-6). ^{31}P NMR (D_2O): δ −24.55 (m), −12.83 (m), −12.43 (m). HRMS *m*/*z*: found 694.9720 $(M - H^+)^-$. $C_{14}H_{23}N_2O_{22}P_4$ requires 694.9693. Purity, >99% by HPLC (system A, 18.6 min; system C, 7.1 min).

Molecular Modeling. The published molecular model of the human $P2Y_2$ receptor[1] was updated by insertion of a part of the C-terminal (CT) domain including the H8 helix and the N-terminal (NT) domain. The $P2Y_2$ CT domain (residues Gly310−Met346) was modeled by homology to bovine rhodopsin. We used the published sequence alignment[1] to superimpose the backbone atoms of the TM domain of the $P2Y_2$ receptor on the corresponding atoms of bovine rhodopsin (PDB code 1U19)[33] with Sybyl 7.1.[34] The rhodopsin TM domains and its hydrophilic loops (Ala26−Met309) as well as Gly310 of the $P2Y_2$ receptor (last residue in the published model) subsequently were removed from the receptor structures. The remaining rhodopsin NT (Met1−Glu25) and CT (residues starting from Asn310) domains were connected to Gly22 and Ala309 of the $P2Y_2$ receptor, respectively. The residues of the CT domain were replaced with the corresponding residues of the $P2Y_2$ receptor (residues Gly310−Met346) with Sybyl 7.1.

An attempt to apply the same technique for modeling of the NT domain failed because of overlap of the rhodopsin NT domain and the extracellular loops (ELs) of the $P2Y_2$ receptor. For this reason, the configuration of the $P2Y_2$ receptor NT domain (Met1−Gly22)

was predicted with the Loopy program from the Jackal package[35] and 1000 initial conformations were generated. The option of energy minimization of the generated candidates was used.

The $P2Y_2$ receptor model was minimized with Sybyl 7.1 in the Amber7 FF99 force field. The energy minimization of side chains of the terminal domains initially was performed with constrained positions of all other atoms of the $P2Y_2$ receptor until an energy gradient lower than 0.05 kcal·mol^{-1}·Å^{-1} was reached. The minimization was continued without any constraints in the terminal domains but with constraint of the atoms of the TM helices and hydrophilic loops. The structure was then minimized, fixing only the backbone atoms of the TM α-helices until an energy gradient lower than 0.05 kcal·mol^{-1}·Å^{-1} was reached. Finally, an unconstrained energy minimization of the whole $P2Y_2$ receptor model was performed until the energy gradient was lower than 0.05 kcal·mol^{-1}·Å^{-1}. The formal geometry of the model was tested with the ProTable command of Sybyl 7.1 as well as the Procheck software.[18]

Molecular Dynamics Simulation of the $P2Y_2$ Receptor. The molecular dynamics (MD) simulation of the $P2Y_2$ receptor was performed on the NIH Biowulf Cluster (Bethesda, MD) with CHARMM 32a2 software.[36] The protocol used for the system construction and MD simulation was described previously.[18,37] The constructed system included the $P2Y_2$ receptor surrounded by 100 DOPC lipids, 5964 TIP3 water molecules, and 107 Cl^- and K^+ ions, for a total of 37 242 atoms. The MD simulation was performed for 10 ns under conditions of CPT (constant pressure and temperature), as previously described.[18] A hexagonal unit cell (69.3 Å × 69.3 Å × 85 Å) and hexagonal periodic boundary conditions in all directions were used.

For the first 4.5 ns of MD simulation, nuclear Overhauser effect (NOE) restraints were applied within TM7 to the distances between each backbone carbonyl oxygen atom of residue *n* and the backbone NH group of the residue $n + 4$. The restraints were applied to all residues of TM7 with the exception of prolines and residues before and after prolines. MD simulation performed without such restraints led to a disordered secondary structure of TM7. Similar findings were described previously for the $P2Y_6$ receptor.[18] After 4.5 ns, the MD simulation was continued without any restraints and the helical structure of the TM7 remained stable until the end of the simulation. The typical structure of the $P2Y_2$ receptor calculated from the last 100 ps of the MD trajectory was used as the final model.

Manual Molecular Docking. The structure of UTP containing all hydrogen atoms initially was sketched with Sybyl 7.1. The ligand geometry was optimized in the Tripos force field with Gasteiger−Hückel atomic charges.[34] Available site-directed mutagenesis data and previously published results of molecular modeling[1,13,18] were used (with the DOCK command of the Sybyl 7.1 package[34]) to manually preposition UTP (with an anti conformation of the uracil ring and an (N)-conformation of the ribose ring) inside the putative binding site of the $P2Y_2$ receptor. The triphosphate chain of the ligand was placed between the R3.29, R6.55, and R7.39. The nucleobase ring was located near Y1.39, Y2.53, and S7.43.

The manual molecular docking procedure was performed in several stages. During the first stage of the molecular docking process, only the bonds of the ligand were flexible. When the most energetically favorable location and conformation of the ligand were found, the molecular docking procedure was repeated with flexible bonds of the receptor. During each iteration of the docking process, the minimization of the binding site with the ligand inside was performed until an rms of 0.01 kcal·mol^{-1}·Å^{-1} was reached. Finally, the energy of the entire obtained protein−ligand complex was minimized until an energy gradient lower than 0.01 kcal·mol^{-1}·Å^{-1} was reached.

Conformational Analysis of UTP, ATP, and Their Derivatives. The conformational analysis of the studied mononucleotides located in the putative binding site of the $P2Y_2$ receptor was performed with the MCMM and the mixed torsional/low-mode sampling methods implemented in the MacroModel 9.0 software.[38] MCMM calculations initially were performed for UTP and all residues located within 5 Å of the ligand, with a shell of constrained atoms with a radius of 2 Å. The following parameters were used: MMFFs force field, water as an implicit solvent, maximum of 1000 iterations of the Polak−Ribier conjugate gradient (PRCG) minimization method with a convergence threshold of 0.05 kJ·mol^{-1}·Å^{-1}, number of conformational search steps = 100, energy window for saving structures = 1000 kJ·mol^{-1}. The ligand−receptor complex obtained after MCMM calculations was subjected to an additional 100 steps of the mixed torsional/low-mode conformational search. The structure of UTP docked in the receptor subsequently was transformed to other studied UTP analogues by substitution of functionalities, and MCMM calculations were performed for each analogue, setting the number of steps to 100 and the energy window for saving structures to 100 kJ·mol^{-1}.

Molecular Docking of Up_4U. The "subsequent ligand composition" technique was introduced to dock the dinucleotide Up_4U to the $P2Y_2$ receptor. The UTP binding mode obtained after MCMM calculations was used as a starting point. Initially, the δ-phosphate group was added to UTP located inside the receptor. The resulting uridine 5′-tetraphosphate and all residues located within 5 Å of the ligand were subjected to MCMM calculations with a shell of constrained atoms within a radius of 2 Å. The following parameters were used: MMFFs force field, water as an implicit solvent, maximum of 1000 iterations of the (PRCG) minimization method with a convergence threshold of 0.05 kJ·mol^{-1}·Å^{-1}, number of conformational search steps = 100, energy window for saving structures = 100 kJ·mol^{-1}. A ribose moiety in its (N)-conformation was then attached to the δ-phosphate group of the ligand. The obtained molecule and all residues located within 5 Å were also subjected to MCMM calculations with the same parameters. The uracil ring in its anti conformation then was attached to the ligand. The resulting Up_4U and all receptor residues located within 5 Å from the ligand were subjected to MCMM calculations with the specified parameters. Finally, Up_4U and all receptor residues located within 5 Å of the ligand were subjected to an additional 100 steps of the mixed torsional/low-mode conformational search.

Acknowledgment. Mass spectral measurements were carried out by John Lloyd, and NMR measurements were carried out by Wesley White (NIDDK). This research was supported in part by the Intramural Research Program of the NIH, National Institute of Diabetes and Digestive and Kidney Diseases. This work was supported by National Institutes of Health Grants GM38213 and HL34322 to T. K. Harden. We thank C. Hoffmann (University of Würzburg, Germany) and C. Müller and A. El-Tayeb (University of Bonn, Germany) for helpful discussions.

Supporting Information Available: Details on the $P2Y_2$ receptor model geometry; details on selective recognition; additional references; figures illustrating the change in energy and rmsd of the $P2Y_2$ receptor during the MD simulation, UDP and Up_4U docked inside the $P2Y_2$ receptor, and UTP docked in a $P2Y_2/P2Y_6$ chimeric receptor; and purity data of target compounds. This material is available free of charge via the Internet at http://pubs.acs.org.

References

(1) Costanzi, S.; Mamedova, L.; Gao, Z. G.; Jacobson, K. A. Architecture of P2Y nucleotide receptors: Structural comparison based on sequence analysis, mutagenesis, and homology modeling. *J. Med. Chem.* **2004**, *47*, 5393−5404.
(2) Brunschweiger, A.; Müller, C. E. P2 receptors activated by uracil nucleotides−an update. *Curr. Med. Chem.* **2006**, *13*, 289−312.
(3) Jacobson, K. A.; Jarvis, M. F.; Williams, M. Purine and pyrimidine (P2) receptors as drug targets. *J. Med. Chem.* **2002**, *45*, 4057−4093.
(4) Jacobson, K. A.; Costanzi, S.; Ohno, M.; Joshi, B. V.; Besada, P.; Xu, B.; Tchilibon, S. Molecular recognition at purine and pyrimidine nucleotide (P2) receptors. *Curr. Top. Med. Chem.* **2004**, *4*, 805−819.
(5) Jacobson, K. A.; Mamedova, L.; Joshi, B. V.; Besada, P.; Costanzi, S. Molecular recognition at adenine nucleotide (P2) receptors in platelets. *Semin. Thromb. Hemostasis* **2005**, *31*, 205−216.

(6) Lustig, K. D.; Shiau, A. K.; Brake, A. J.; Julius, D. Expression cloning of an ATP receptor from mouse neuroblasoma cells. *Proc. Natl. Acad. Sci. U.S.A.* **1993**, *90*, 5113−5117.
(7) Arthur, D. B.; Georgi, S.; Akassoglou, K.; Insel, P. A. Inhibition of apoptosis by $P2Y_2$ receptor activation: novel pathways for neuronal survival. *J. Neurosci.* **2006**, *26*, 3798−3804.
(8) Bagchi, S.; Liao, Z.; Gonzalez, F. A.; Chorna, N. E.; Seye, C. I.; Weisman, G. A.; Erb, L. The $P2Y_2$ nucleotide receptor requires interaction with α_v integrins to communicate with G_α and stimulate chemotaxis. *J. Biol. Chem.* **2005**, *280*, 39058−39066.
(9) Camden, J. M.; Schrader, A. M.; Camden, R. E.; González, F. A.; Erb, L.; Seye, C. I.; Weisman G. A. $P2Y_2$ nucleotide receptors enhance α-secretase-dependent amyloid precursor protein processing. *J. Biol. Chem.* **2005**, *280*, 18696−18702.
(10) Davis, B. M.; Malin, S. A.; Koerber, H. R.; Albers, K. M.; Koller, B. H.; Molliver, D. C. Mice Lacking the $P2Y_2$ Receptor Have Deficits in Noxious Thermal Sensation and Neuronal Responses to Capsaicin. Presented at the National Meeting of the Society for Neuroscience, 2005; Abstract 393.16.
(11) Yerxa, B. R.; Sabater, J. R.; Davis, C. W.; Stutts, M. J.; Lang-Furr, M.; Picher, M.; Jones, A. C.; Cowlen, M.; Dougherty, R.; Boyer, J.; Abraham, W. M.; Boucher, R. C. Pharmacology of INS37217 [P(1)-(uridine 5′)-P(4)-(2′-deoxycytidine 5′-tetraphosphate, tetrasodium salt], a next-generation $P2Y_2$ receptor agonist for the treatment of cystic fibrosis. *J. Pharmacol. Exp. Ther.* **2002**, *302*, 871−880.
(12) Kellerman, D.; Evans, R.; Mathews, D.; Shaffer, C. Inhaled $P2Y_2$ receptor agonists as a treatment for patients with cystic fibrosis lung disease. *Adv. Drug Delivery Rev.* **2002**, *54*, 1463−1474.
(13) Jacobson, K. A.; Costanzi, S.; Ivanov, A. A.; Tchilibon, S.; Besada, P.; Gao, Z. G.; Maddileti, S.; Harden, T. K. Structure activity and molecular modeling analyses of ribose- and base-modified uridine 5′-triphosphate analogues at the human $P2Y_2$ and $P2Y_4$ receptors. *Biochem. Pharmacol.* **2006**, *71*, 540−549.
(14) Malmsjö, M.; Adner, M.; Harden, T. K.; Pendergast, W.; Edvinsson, L.; Erlinge, D. The stable pyrimidines $UDP_\beta S$ and $UTP_\gamma S$ discriminate between the P2 receptors that mediate vascular contraction and relaxation of the rat mesenteric artery. *Br. J. Pharmacol.* **2000**, *131*, 51−56.
(15) Erb, L.; Garrad, R.; Wang, Y.; Quinn, T.; Turner, J. T.; Weisman, G. A. Site-directed mutagenesis of P_{2U} purinoceptors. *J. Biol. Chem.* **1995**, *270*, 4185−4188.
(16) Laskowski, R. A.; MacArthur, M. W.; Moss, D. S.; Thornton, J. M. PROCHECK: A program to check the stereochemical quality of protein structures. *J. Appl. Crystallogr.* **1993**, *26*, 283−291.
(17) Mehler, E. L.; Periole, X.; Hassan, S. A.; Weinstein, H. Key issues in the computational simulation of GPCR function: representation of loop domains. *J. Comput.-Aided Mol. Des.* **2002**, *16*, 841−853.
(18) Costanzi, S.; Joshi, B. V.; Maddileti, S.; Mamedova, L.; Gonzalez-Moa, M. J.; Marquez, V. E.; Harden, T. K.; Jacobson, K. A. Human $P2Y_6$ receptor: Molecular modeling leads to the rational design of a novel agonist based on a unique conformational preference. *J. Med. Chem.* **2005**, *48*, 8108−8111.
(19) Ballesteros, J. A.; Shi, L.; Javitch, A. Structural mimicry in G protein-coupled receptors: implications of the high-resolution structure of rhodopsin for structure−function analysis of rhodopsin-like receptors. *Mol. Pharmacol.* **2001**, *60*, 1−19.
(20) Yu, H.; Oprian, D. D. Tertiary interactions between transmembrane segments 3 and 5 near the cytoplasmic side of rhodopsin. *Biochemistry* **1999**, *38*, 12033−12040.
(21) Kim, H. S.; Ravi, R. G.; Marquez, V. E.; Maddileti, S.; Wihlborg, A.-K.; Erlinge, D.; Malmsjö, M.; Boyer, J. L.; Harden, T. K.; Jacobson, K. A. Methanocarba modification of uracil and adenine nucleotides: High potency of Northen ring conformation at $P2Y_1$, $P2Y_2$, $P2Y_4$, and $P2Y_{11}$, but not $P2Y_6$ receptors. *J. Med. Chem.* **2002**, *45*, 208−218.
(22) Meyer, E. A.; Castellano, R. K.; Diederich, F. Interactions with aromatic rings in chemical and biological recognition. *Angew. Chem., Int. Ed.* **2003**, *42*, 1210−1250.
(23) Shaver, S. R.; Rideout, J. L.; Pendergast, W.; Douglass, J. G.; Brown, E. G.; Boyer, J. L.; Patel, R. I.; Redick, C. C.; Jones, A. C.; Picher, M.; Yerxa, B. R. Structure−activity relationships of dinucleotides: potent and selective agonists of P2Y receptors. *Purinergic Signalling* **2005**, *1*, 183−191.
(24) Pendergast, W.; Yerxa, B. R.; Douglass, J. G.; Shaver, S. R.; Dougherty, R. W.; Redick, C. C.; Sims, I. F.; Rideout, J. L. Synthesis and P2Y receptor activity of a series of uridine dinucleotides 5′-polyphosphates. *Bioorg. Med. Chem. Lett.* **2001**, *11*, 157−160.
(25) Fradera, X.; Mestres, J. Guided docking approaches to structure-based design and screening. *Curr. Top. Med. Chem.* **2004**, *4*, 687−700.
(26) El-Tayeb, A.; Qi, A.; Müller, C. E. Synthesis and structure−activity relationships of uracil nucleotide derivatives and analogues as agonists at the human $P2Y_2$, $P2Y_4$, and $P2Y_6$ receptors. *J. Med. Chem.* **2006**, *49*, 7076−7087.
(27) Verheyden, J. P. H.; Wagner, D.; Moffatt, J. G. Synthesis of some pyrimidine 2′-amino-2′-deoxynucleosides. *J. Org. Chem.* **1971**, *36*, 250−254.
(28) Rajeev, K. G.; Prakash, T. P.; Manoharan, M. 2′-Modified-2-thiothymidine oligonucleotides. *Org. Lett.* **2003**, *5*, 3005−3008.
(29) Halbfinger, E.; Major, D. T.; Ritzmann, M.; Ubl, J.; Reiser, G.; Boyer, J. L.; Harden, K. T.; Fischer, B. Molecular recognition of modified adenine nucleotides by the $P2Y_1$-receptor. 1. A synthetic, biochemical, and NMR approach. *J. Med. Chem.* **1999**, *42*, 5325 − 5337.
(30) Nicholas, R. A.; Lazarowski, E. R.; Watt, W. C.; Li, Q.; Harden, T. K. Uridine nucleotide selectivity of three phospholipase C-activating P2 receptors: Identification of a UDP-selective, a UTP-selective, and an ATP- and UTP-specific receptor. *Mol. Pharmacol.* **1996**, *50*, 224−229.
(31) Brown, H. A.; Lazarowski, E. R.; Boucher, R. C.; Harden, T. K. Evidence that UTP and ATP regulate phospholipase C through a common extracellular 5′-nucleotide receptor in human airway epithelial cells. *Mol. Pharmacol.* **1991**, *40*, 648−655.
(32) Poznanski, J.; Felczak, K.; Kulikowski, T.; Remin, M. ^{1}H NMR conformational study of antiherpetic C5-substituted 2′-deoxyuridines: insight into the nature of structure−activity relationships. *Biochem. Biophys. Res. Commun.* **2000**, *272*, 64−74.
(33) Okada, T.; Sugihara, M.; Bondar, A. N.; Elstner, M.; Entel, P.; Buss, V. The retinal conformation and its environment in rhodopsin in light of a new 2.2 Å crystal structure. *J. Mol. Biol.* **2004**, *342*, 571−583.
(34) *Sybyl*, version 7.1; Tripos Inc. (1699 South Hanley Road, St. Louis, Missouri, 63144).
(35) URL: http://honiglab.cpmc.columbia.edu/programs/jackal/intro.html.
(36) Brooks, B. R.; Bruccoleri, R. E.; Olafson, B. D.; States, D. J.; Swaminathan, S.; Karplus, M. CHARMM, a program for macromolecular energy, minimization, and dynamics calculations. *J. Comput. Chem.* **1983**, *4*, 187−217.
(37) Woolf, T. B.; Roux, B. Structure, energetics, and dynamics of lipid−protein interactions: A molecular dynamics study of the gramicidin A channel in a DMPC bilayer. *Proteins* **1996**, *24*, 92−114.
(38) Mohamadi, F. N.; Richards, G. J.; Guida, W. C.; Liskamp, R.; Lipton, M.; Caufield, C.; Chang, G.; Hendrickson, T.; Still, W. C. Macro-Model, an integrated software system for modeling organic and bioorganic molecules using molecular mechanics. *J. Comput. Chem.* **1990**, *11*, 440−467.
(39) Šponer, J.; Leszczynski, J.; Hobza, P. Thioguanine and thiouracil: hydrogen-bonding and stacking properties. *J. Phys. Chem. A* **1997**, *101*, 9489−9495.
(40) Verheyden, J. P. H.; Wagner, D.; Moffatt, J. G. Synthesis of some pyrimidine 2′-amino-2′-deoxynucleosides. *J. Org. Chem.* **1971**, *36*, 250−245.
(41) Aurup, H.; Tuschl, T.; Benseler, F.; Ludwig, J.; Eckstein, F. Oligonucleotide duplexes containing 2′-amino-2′-deoxycytidines: thermal stability and chemical reactivity. *Nucleic Acids Res.* **1994**, *22*, 20−24.
(42) Lazarowski, E. R.; Watt, W. C.; Stutts, M. J.; Brown, H. A.; Boucher, R. C.; Harden, T. K. Enzymatic synthesis of UTP gamma S, a potent hydrolysis resistant agonist of the P_{2U}-purinoceptors. *Br. J. Pharmacol.* **1996**, *117*, 203−209.

JM060903O